Environmental Science Processes & Impacts

ROYAL SOCIETY OF CHEMISTRY

PAPER

View Article Online
View Journal | View Issue

Cite this: *Environ. Sci.: Processes Impacts*, 2025, **27**, 2262

Virulence gene profiling and cytotoxicity of *Vibrio* spp. isolated from treated wastewater effluent and receiving surface waters in Durban, South Africa†

Kerisha Ramessar and Ademola O. Olaniran *

Untreated or partially treated wastewater often harbours virulent *Vibrio* species that threaten environmental and public health. This study aimed to characterize the virulence gene profiles and cytotoxic effects of *Vibrio* species isolated from treated effluents and downstream rivers at four wastewater facilities in Durban, KwaZulu-Natal province, South Africa. A total of 200 *Vibrio* spp., isolated from treated effluent and surface waters of four wastewater treatment facilities in Durban, KwaZulu-Natal, were screened, with *Vibrio vulnificus* isolates ($n = 178$) showing high prevalence of iron acquisition genes such as *viuB* (72.47%), *feoB* (56.74%) and *fbpC* (55.06%) while other virulence genes like *ompU*, *apxIB*, and *hlyB* were also detected. *Vibrio alginolyticus* isolates ($n = 15$) exhibited *rtx* (66.67%) and *pvuA* (46.67%), among others. Five representative isolates caused a progressive decline in cell viability in both HepG2 and HEK293 cells over 72 h, with final viability dropping below 3% in multiple instances. Morphological damage confirmed strong cytotoxic activity. Statistical analysis showed significant associations between specific genes detected among the isolates. These findings demonstrate that treated wastewater still contains highly virulent *Vibrio* strains capable of harming human cells, posing ongoing risks in regions with compromised water infrastructure.

Received 1st February 2025
Accepted 30th June 2025

DOI: 10.1039/d5em00083a

rsc.li/espi

Environmental significance

Wastewater treatment plants are vital for reducing microbial contamination in aquatic environments. The persistence of pathogenic bacteria such as *Vibrio* spp. in treated wastewater effluents and environmental waters is a public health concern. Consequently, this study profiled virulence genes in 200 *Vibrio* spp. isolates obtained from treated effluent and surface waters at four wastewater treatment plants in Durban, KwaZulu-Natal. Additionally, the cytopathic effects of five selected isolates were assessed in HepG2 and HEK293 cell lines. The results reveal the presence of various virulence genes among *Vibrio* spp., their significant associations, and the isolates' strong cytotoxic effects on human cells. These findings emphasize the need for continuous monitoring and improvement of wastewater treatment processes to effectively eradicate pathogenic bacteria.

1. Introduction

The global burden of waterborne diseases remains a pressing concern, driven largely by the discharge of inadequately treated wastewater into surface waters, which serves as a conduit for pathogenic microorganisms. This scenario poses severe public health threats, particularly in communities that depend on these contaminated water bodies for domestic purposes.[1–3] The challenge is most acute in developing regions where wastewater infrastructure is often under-resourced or poorly maintained.[4] South Africa exemplifies this crisis, with an estimated 40 to 50% of its 1400 wastewater treatment facilities failing to meet acceptable operational standards.[3] Although existing studies have documented the occurrence of pathogenic bacteria in treated effluents,[5,6] limited attention has been given to the virulence potential and cytotoxicity of *Vibrio* species within these systems. This gap is concerning, considering the growing recognition of *Vibrio* spp. as significant environmental and clinical pathogens.

Vibrio species are Gram-negative, facultatively anaerobic bacteria belonging to the Vibrionaceae family and are increasingly identified as threats in wastewater-contaminated aquatic ecosystems.[7] Pathogenic strains of *Vibrio* have been documented in treated effluents from wastewater treatment plants (WWTPs) in the Eastern Cape of South Africa and other areas.[2] Among the 147 recognized species, twelve are known to cause disease in humans.[8] Notable among these are *Vibrio cholerae*, which accounted for over 1.2 million cases, globally, in 2017,[9] *V. vulnificus*, associated with severe septicaemia and high mortality rates,[10] and *V. alginolyticus*, implicated in wound infections and otitis.[11,12] The pathogenicity of these organisms

Discipline of Microbiology, School of Life Sciences, University of KwaZulu-Natal (Westville Campus), Durban, 4000, South Africa. E-mail: olanirana@ukzn.ac.za; Tel: +27-31-260-7400

† Electronic supplementary information (ESI) available. See DOI: https://doi.org/10.1039/d5em00083a

is attributed to a suite of virulence factors, including iron acquisition systems such as *viuB*, *feoB*, and *fbpC*, cytolytic hemolysins (*hlyA–D*), adhesion and colonization factors like *ompU* and *tcp*; and motility-related flagellin genes (*flaA–C*).[13–21] These virulence determinants not only facilitate environmental persistence but also enhance host invasion and tissue damage, underscoring the need for targeted surveillance of *Vibrio* spp. in treated effluents.

While previous studies have documented the presence of pathogenic *Vibrio* spp. in wastewater effluents and receiving surface waters in South Africa,[2,6] there remains a critical gap in understanding the virulence potential of these strains in treated waters and their implications for human health. This study uniquely addresses this gap by combining molecular profiling of virulence genes with statistical correlation analyses to elucidate the pathogenicity of *Vibrio* isolates from wastewater effluents. Additionally, we investigate the cytopathic effects of selected *V. vulnificus* strains on human hepatoblastoma (HepG2) and human embryonic kidney (HEK) cell lines, providing novel insights into their potential health risks upon exposure.

While most prior research has focused on marine or clinical isolates of *Vibrio*, our study addresses a critical gap by investigating strains that persist through municipal wastewater treatment processes and their receiving surface waters. We hypothesize that these environmental isolates harbour enriched virulence gene repertoires and exhibit heightened cytotoxicity toward human cells. Ultimately, this approach offers novel insights into the environmental persistence and health risk potential of *Vibrio* spp., with direct implications for water quality monitoring and public health policy in resource-limited settings.

2. Materials and methods

2.1 Isolation and molecular identification of the *Vibrio* isolates

Wastewater samples were obtained from four wastewater treatment facilities in Durban, KwaZulu-Natal, South Africa. The geographical coordinates of the four wastewater treatment plants are 29°47′43″S 30°59′52″E (WWTP1), 29°40′43″S 31° 02′01″E (WWTP2), 29°59′25″S 30°54′21″E (WWTP3), and 29° 50′42″S 30°53′27″E (WWTP4). Samples were collected seasonally from various locations at each wastewater treatment plant (WWTP), including (1) influent, (2) pre-chlorination, (3) activated sludge or biofilter, (4) post-chlorination, (5) upstream, and (6) downstream of the receiving rivers, during the sampling period from September 2020 to August 2021. Samples were collected in 5 L sterile bottles, subsequently carried on ice to the University of KwaZulu-Natal (Westville campus), where they were maintained at 4 °C and analysed within 48 h of collection. The materials underwent serial dilution with sterile distilled water and were subsequently filtered using a 0.45 μm cellulose nitrate filter. The filters were applied to thiosulfate-citrate-bile salts-sucrose agar (Sigma-Aldrich, St. Louis, MO, USA) and incubated at 37 °C for 24 h. Green and yellow colonies were recognized as probable *Vibrio* isolates. Two hundred putative *Vibrio* spp. were isolated from the treated effluents, as well as from upstream and downstream locations of the river. PCR amplification of the *V16s* housekeeping gene was conducted to verify the identity of the organisms as *Vibrio* spp. utilizing the primers *V16s-700F*: CGGTGAAATGCGTAGAGAT and *V16s-1325R*: TTACTAGCGATTCCGAGTTC.[22] Species identification for *V. vulnificus* was conducted utilizing the primers *Vv.hsp-326F*: GTCTTAAAGCGGTTGCTGC and *Vv.hsp-697R*: CGCTTCAAGTGCTGGTAGAAG.[22] A semi-nested PCR was conducted to identify *V. alginolyticus* using the primers: *VA16F1*: ATTGAAGAGTTTGATCATGGCTCAGA, *VA16F2*: CCTTCGGGTTGTAAAGCACT, and *VA16R2*: TCCTCCCGTAGTTGAAACTACCT.[23]

2.2 Virulence gene profiling of *Vibrio* spp.

Detection of virulence genes in *V. vulnificus*, *V. alginolyticus*, and *Vibrio* spp. was conducted by monoplex PCR. Primers for the virulence genes were developed utilizing the DNA sequences from *V. vulnificus* (ATCC 27562) and *V. alginolyticus* (ATCC 17749) received from NCBI GenBank (**https://www.ncbi.nlm.nih.gov/**) and were subsequently extracted and aligned for the specific virulence genes. The primer-BLAST tool facilitated primer design, and the resulting primers (Table 1) were manufactured by Inqaba Biotech, Pretoria, South Africa. *V. vulnificus* was screened for *apxIB*, *fbpC*, *feoB*, *ompU*, *sodB*, *tldD*, *viuB*, and *hlyB*, whereas *V. alginolyticus* was checked for *asp*, *pvuA*, *tlh*, and *rtx*. All amplifications were conducted in 25 μL reactions, comprising 12.5 μL of 2× master mix (Thermo-Fisher, Waltham, MA, USA), 0.2 μM of each primer, 12 μL of nuclease-free water, and 2 μL of

Table 1 Primers used for virulence genes profiling

Target gene	Sequence (5′–3′)	Product length (bp)	Annealing temperature
apxIB	F: GCCAACTGCGTGATGTGTTT R: ATTTGGCCGGTTTGACGTTG	298	55.7 °C for 60 s
fbpC	F: GGAAGTGGAACAAGGGCAGA R: TCAGGTGGAACCCAATGCTC	159	62.8 °C for 60 s
feoB	F: AAGCGTTTCGTTTTGGGAGC R: ACCAACTACCGCCTCTTTGG	237	64.3 °C for 40 s
ompU	F: TGGCGTCTGTCATCGTTTCA R: ACCAGCACCGTTATCACCTG	254	55.7 °C for 60 s
sodB	F: TTGAGTTCCACCACGGCAAA R: GTGATTGGTGTTGCCGCATT	370	58 °C for 40 s
tldD	F: GGCAACAAACGCTGTAGCTC R: CATGTCTTTGCCCACCATGC	766	64.3 °C for 40 s
viuB	F: GCCTGAACACAAACCCGTTC R: CCGCGATAAAAGCAGACAGC	449	62.8 °C for 60 s
hlyB	F: GAACGCGAGTAAATCACGCC R: AAGCGCACGTTATCGAATGC	481	58 °C for 40 s
asp	F: AGACCGCATGTCTGGTTTGT R: GCTCAATACTCTCACGCCGA	475	64.3 °C for 30 s
pvuA	F: GATGCGCCGCTGAATGATTT R: CACTGTCGGCAAATGGCAAA	343	64.3 °C for 30 s
tlh	F: GTGGTTAGCGCGCAAGAAAA R: GGTGCTTTGGTTGCATCAGG	770	64.3 °C for 30 s
rtx	F: CCGACAGCTTGTTTGTTGGG R: CACGTCAACACCGTCTGGTA	473	64.3 °C for 30 s

template DNA. The PCR cycling parameters for *V. vulnificus* genes consist of an initial denaturation at 96 °C for 5 min, succeeded by 35 cycles of 94 °C for 60 s, annealing (refer to Table 1), and 72 °C for 60 s, culminating in a final extension at 72 °C for 7 min. The PCR cycling parameters for *V. alginolyticus* genes consist of an initial denaturation at 93 °C for 15 min, succeeded by 35 cycles of denaturation at 92 °C for 40 s, annealing (Table 1), elongation at 72 °C for 1 min and 30 s, and a final elongation step at 72 °C for 7 min following the completion of 30 cycles. PCR products were resolved using gel electrophoresis at 100 V for 45 min on a 1.5% agarose gel, stained with 5 μg mL^{-1} ethidium bromide, and visualized under a UV transilluminator utilizing the Chemigenius Bioimaging System (Syngene, Cambridge, UK). The multi-virulence gene index (MVGI) was computed using the following equation MVGI = VGD/VGT[24] where VGD denotes the virulence genes found, and VGT signifies the total number of virulence genes.

2.3 Cytotoxicity assays

Human embryonic kidney (HEK293) and human hepatoblastoma (HepG2) cells were cultured in tissue culture (T25) flasks using Dulbecco's modified Eagle's medium (DMEM), supplemented with 10% fetal bovine serum and 1% penicillin–streptomycin (ThermoFisher, Waltham, MA, USA), and incubated at 37 °C in 5% carbon dioxide.

2.3.1 Treatment concentration selection and rationale. The treatment concentration of 1.5×10^8 CFU mL^{-1} was selected based on established protocols for evaluating *Vibrio* cytotoxicity[25,26] and previous studies assessing similar pathogenic mechanisms.[27,28] This standardized concentration ensures direct comparability with established research and supports cross-study comparisons of *Vibrio* virulence and cytotoxicity. Although this concentration exceeds typical levels found in treated wastewater (10^3–10^4 CFU mL^{-1}), it is representative of potential bacterial loads encountered in biofilms, during bloom conditions, or peak exposure events in coastal and estuarine waters.[29]

The selected concentration balances several critical factors: (1) ecological relevance by reflecting potential environmental exposures, (2) reproducibility across experimental replicates, and (3) generation of measurable cytotoxic effects suitable for quantitative analysis. Furthermore, *in vitro* infection models commonly employ similar concentrations to assess bacterial cytotoxicity and virulence factor activity.[30,31]

To validate that the cytotoxic effects were attributable to virulence factors rather than the bacterial load alone, additional dose-response experiments were performed. Serial dilutions of *V. vulnificus* suspensions, ranging from 10^0 to 10^{-6}, were prepared and used to treat HepG2 and HEK293 cells. Cell viability was then assessed following exposure to each dilution to observe changes in cytotoxicity.

2.3.2 MTT viability assay. The MTT (3-(4,5-dimethylthiazol-2-yl)-2,5-diphenyltetrazolium bromide) assay is a colorimetric assay used to assess the percentage of cell viability after exposure of *V. vulnificus* on HEK293 and HepG2 cells. After 75% confluence was achieved, the cells were removed from the flask using trypsin and resuspended in DMEM, with 100 μL aliquots planted into each well (2×10^5 cells per well) of a 96-well microtiter plate. Following incubation at 37 °C for 24 h, the medium was replaced with 180 μL of fresh DMEM. Five *V. vulnificus* strains (V.v.137, V.v.406, V.v.419, V.v.420, and V.v.444) were selected for this assay based on their antibiograms (data not shown) and distinct virulence gene profiles (Table S1†). In addition to their high antibiotic resistance and virulence potential, these five isolates exhibited unique combinations of antibiotic resistance and virulence gene profiles compared to the rest of the isolates in this study. This made them valuable for assessing the risks they may pose to human health and for informing future treatment strategies.

Bacterial cells were cultured in nutritional broth to mid-log phase and centrifuged, the pellet was rinsed with phosphate-buffered saline (pH 7.4) and standardized to approximately 1.5×10^8 cells per mL using DMEM.

Twenty microliters of the standardized bacterial suspension were applied to each well of the 96-well microtiter plate and incubated for 24, 48, and 72 h. Uninfected cells were used as a negative control, whereas *V. vulnificus* ATCC 27562 served as a positive control. Each experimental condition was performed in triplicate (three technical replicates), and each experiment was repeated three times independently (three biological replicates) to ensure reproducibility and statistical reliability.

Following incubation of *V. vulnificus* with the cells, 20 μL of MTT (1 mg mL^{-1}) was introduced to each well and incubated for 3 h at 37 °C in 5% carbon dioxide. Following incubation, the supernatant was carefully removed, and 100 μL of pure dimethyl sulfoxide (DMSO) was introduced to the wells to solubilize the purple formazan crystals that developed in the cell cytoplasm. Optical absorbance was measured with the plate reader at 570 nm.

It is hypothesized that differential cytotoxic responses between HepG2 and HEK-293 cells may result from their distinct cellular origins, with HepG2 cells (liver-derived) potentially exhibiting different detoxification mechanisms and cellular defence pathways compared to HEK-293 cells (kidney-derived), leading to varying susceptibilities to *V. vulnificus* virulence factors.

2.4 Evaluation of cell morphology

The cell morphology and overall health of HepG2 and HEK293 cells were assessed by capturing multiple field views for each experimental condition using the Invitrogen EVOS FLoid EN61326 high-resolution microscope, which is equipped with phase-contrast and fluorescence capabilities that ensured a representative and detailed analysis (ThermoFisher Scientific, Waltham, MA, USA).

2.5 Statistics

The associations between various virulence genes among isolates were assessed by comparing Pearson chi-square values (χ^2), determined using descriptive analysis of crosstabs for contingency tables, at a significance level of $p < 0.05$. Furthermore, the odds ratio (OR) for each pair of virulence genes was

employed to measure the intensity of their correlation. An odds ratio (OR) greater than 1 indicates a positive correlation, implying that the presence of one gene enhances the likelihood of the other being present; an OR less than 1 indicates a negative association, while an OR equal to 1 shows no association.[32] Analyses were conducted using IBM SPSS Statistics 28.0. The cytotoxicity results were analysed using a completely randomized design (CRD) with three replicates. The data underwent analysis of variance, and means were differentiated using the Tukey test at $p \leq 0.0001$. Additionally, certain data were illustrated graphically as mean ± standard deviation.

3. Results

3.1 Virulence gene signatures of the *Vibrio* isolates

Two hundred presumptive *Vibrio* isolates were collected from the discharge point of treated effluent, as well as from upstream and downstream locations of receiving surface waters at four wastewater treatment plants in Durban, KwaZulu-Natal. The isolates were identified as *Vibrio* spp. by PCR amplification of the *Vibrio* 16s rRNA gene. Out of the two hundred isolates, 178 were identified as *Vibrio vulnificus* and 15 as *Vibrio alginolyticus via* PCR amplification of the *Vv.hsp* and *VA16* genes, respectively, while 8 remained unidentifiable at the species level and were categorized as *Vibrio* spp.

PCR amplification of virulence genes: *apxIB*, *ompU*, *sodB*, *hlyB*, *fbpC*, *viuB*, *tldD* and *feoB* demonstrated their presence in some *V. vulnificus* isolates (Fig. 1a, b and Table 2). Out of 178 *V. vulnificus* isolates, *viuB* was discovered in 72.47% ($n = 129$) of isolates, followed by *feoB* in 56.74% ($n = 101$) and *fbpC* in 55.06% ($n = 98$). Furthermore, *ompU* was identified in 35.39% ($n = 63$), *apxIB* in 24.72% ($n = 44$), and *hlyB* in 13.48% ($n = 24$) of the isolates. The *tldD* gene was identified in 6.74% ($n = 12$) of isolates, while *sodB* was identified in 1.69% ($n = 3$) of isolates. Additionally, *asp*, *tlh*, *pvuA,* and *rtx* were identified in certain *V. alginolyticus* isolates.*rtx* was predominantly identified in 66.67% ($n = 10$) of the isolates, while *pvuA* was recognized in 46.67% ($n = 7$) of the isolates. *asp* and *tlh* were identified in 13.33% ($n = 2$) and 6.67% ($n = 1$) of isolates, respectively. In *Vibrio* spp., *viuB* was the most common gene detected in 42.86% (3) of isolates followed by *ompU* and *feoB*, both, detected in 28.57% ($n = 2$) isolates. *fbpC* was only detected in 14.29% ($n = 1$) isolates.

3.2 Virulence genes combinations detected in isolates

Multiple virulence genes were present in all three isolate types: *V. vulnificus*, *V. alginolyticus*, and *Vibrio* spp. (Tables 2 and S1†).

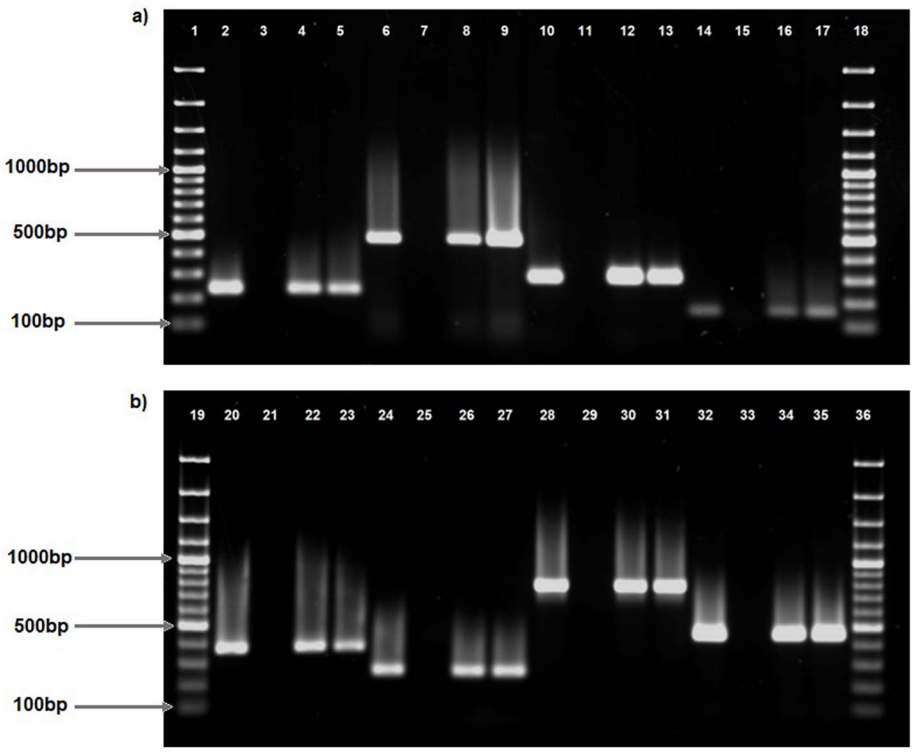

Fig. 1 PCR amplification of virulence genes identified in *V. vulnificus*. Lanes 1, 18, 19, 36, 100bp molecular marker; lane 2, *feoB* positive control (237bp); lane 3, negative control; lanes 4 and 5, positive strains for *feoB* (237bp); lane 6, *hlyB* positive control (481bp); lane 7, negative control; lanes 8 and 9, positive strains for *hlyB* (481bp); lane 10, *apxIB* positive control (291bp); lane 11, negative control; lanes 12 and 13, positive strains for *apxIB* (291bp); lane 14, *fbpC* positive control (159bp); lane 15, negative control; lanes 16 and 17; positive strains for *fbpC* (159bp); lane 20, *sodB* positive control (370bp); lane 21, negative control; lanes 22 and 23; positive strains for *sodB* (370bp); lane 24, *ompU* positive control (254bp); lane 25, negative control; lane 26 and 27, positive strains for *ompU* (254bp); lane 28, *tldD* positive control (766bp); lane 29, negative control; lanes 30 and 31, positive strains for *tldD* (766bp); lane 32, *viuB* positive control (449bp); lane 33, negative control; lane 34 and 35, positive strains for *viuB* (449bp).

Table 2 Number of *V. vulnificus* isolates, *V. alginolyticus* and *Vibrio* spp. harbouring virulence genes

	Virulence genes							
Isolates	*apxIB*	*ompU*	*sodB*	*hlyB*	*fbpC*	*viuB*	*tldD*	*feoB*
V. vulnificus ($n = 178$)	24.72% (44)	35.39% (63)	1.69% (3)	13.48% (24)	55.06% (98)	72.47% (129)	6.74% (12)	56.74% (101)
Vibrio spp. ($n = 7$)	0% (0)	28.57% (2)	0% (0)	0% (0)	14.29% (1)	42.86% (3)	0% (0)	28.57% (2)
	asp		*tlh*		*pvuA*		*rtx*	
V. alginolyticus ($n = 15$)	13.33% (2)		6.67% (1)		46.67% (7)		66.67% (10)	

Six virulence genes (MVGI = 0.75), namely *apxIB*, *ompU*, *hlyB*, *fbpC*, *viuB* and *feoB*, were simultaneously identified in *V. vulnificus* isolates. *apxIB*, *hlyB*, *fbpC*, *viuB*, *tldD* and *feoB* were the predominant virulence genes identified in two samples. Fifteen isolates were reported to contain the presence of five virulence genes (MVGI = 0.625) with the most prevalent pattern of *apxIB*, *ompU*, *fbpC*, *viuB* and *feoB*. Among the thirty-five isolates exhibiting four virulence genes (MVGI = 0.5), ten isolates possessed the combination of *ompU*, *fbpC*, *viuB* and *feoB*; seven isolates included the combination of *apxIB*, *ompU*, *fbpC* and *viuB*; and five isolates included the combination of *hlyB*, *fbpC*, *viuB* and *feoB*. The predominant virulence gene profile identified was *fbpC*, *viuB*, and *feoB*, observed in twenty-five isolates. Furthermore, eleven isolates exhibited the combination of *fbpC* and *viuB*, whereas 10 isolates demonstrated the combination of *viuB* and *feoB*. In *V. alginolyticus*, three virulence genes (MVGI = 0.75) were found in two isolates with combinations of *asp*, *pvuA* and *rtx*, and *asp*, *tlh* and *rtx*. The predominant combination of virulence genes identified was *pvuA* and *rtx*, observed in five isolates. In *Vibrio* spp., two isolates exhibited three virulence genes (MVGI = 0.375): *ompU*, *viuB*, and *feoB*, with *fbpC*, *viuB*, and *feoB* present in each sample. One isolate had a combination of *ompU* and *viuB* (MVGI = 0.25).

3.3 The positive and negative associations of virulence genes detected in isolates

The Pearson χ^2 values at $P < 0.05$ (unless specified otherwise) are derived from cross-tabulation data illustrating the association between the virulence genes in *V. vulnificus*, as shown in Table 3. The data reveal that *viuB* had a significant association with *hlyB* (χ^2: 10.537, OR = 0.682), *fbpC* (χ^2: 50.080, OR = 17.820), *feoB* (χ^2: 32.393, OR = 7.972) and *tldD* (χ^2: 4.888, OR = 1.103). *tldD* exhibited an association with *apxIB* (χ^2: 4.419, OR = 3.368), *ompU* (χ^2: 7.049, OR = 0.896), and *hlyB* (χ^2: 8.762, OR = 5.526). *feoB* demonstrated a strong correlation with *fbpC* (χ^2 16.592, OR = 3.569). *fbpC* had a significant association with *apxIB* (χ^2: 5.601, OR = 2.385) and sodB (χ^2: 6.517, OR = 3.608). The virulence gene *hlyB* revealed a significant relationship with *sodB* (χ^2: 7.399, OR = 13.909). The cross-tabulation results demonstrated a significant correlation between the virulence genes *tlh* and *asp* (χ^2: 6.964, OR = 0.071) in *V. alginolyticus* (Table 3). No positive relationships were discovered between virulence genes detected in *Vibrio* spp. (Table 3).

In *V. vulnificus*, the odds ratio and confidence intervals (CI) indicated relationships (Table 3) involving *viuB* and *fbpC* (OR 17.820, CI: 6.992–45.414), *viuB* and *feoB* (OR 7.92, CI: 3.695–17.202), and *hlyB* and *sodB* (OR 13.909, CI: 1.210–159.851). The elevated OR values indicate a robust correlation between these gene pairs. However, a high confidence interval indicates variability in the data. Robust relationships were identified between *fbpC* and *sodB* (OR 3.608, CI: 1.282–10.151), *ompU* and *apxIB* (OR 3.787, CI: 1.861–7.705), and *fbpC* and *apxIB* (OR 2.385, CI: 1.148–4.952), as indicated by significant associations with confidence intervals that do not include one. Nonetheless, a negligible connection was noted between the gene pairs *rtx* and *asp* (OR 1.250, CI: 0.917–1.704) in *V. alginolyticus*, and *feoB* and *apxIB* (OR 1.004, CI: 0.505–1.997) in *V. vulnificus*, as the odds ratios were proximate to 1 and accompanied by extensive confidence intervals. In the *Vibrio* spp., the odds ratios were approximately one or lower, accompanied by wide confidence intervals, indicating no meaningful connections between the gene pairs.

3.4 Cell morphology of infected and uninfected HEK293 and HepG2 cells

Cytopathic effects of *V. vulnificus* on HEK293 and HepG2 cells are depicted in Fig. 3 and 4, respectively, following infection and incubation with strains V.v.137, V.v.406, V.v.419, V.v.420, V.v.444, positive and negative controls over 24, 48, and 72 h. Prior infection with *V. vulnificus* the HEK293 cells exhibited a spindle morphology (Fig. 3a–g); however, after 24 h of incubation (Fig. 3h–n), the HEK293 cells began to deviate from their characteristic shape and lost their orderly structure. By 48 h (Fig. 3o–u), the cells started to appear rounder in shape and shrivelled, indicating symptoms of cytopathic stress with detachment of cells from the surface of the wells. Following 72 h incubation (Fig. 3v–z, aa, and ab), widespread breakdown of the monolayer was observed with significant distortion of the cells and cell loss being obvious. In HepG2 cells, prior to infection with *V. vulnificus*, cells exhibited an epithelial shape (Fig. 4a–g). At 24 h post-infection, the morphology began transitioning from epithelial shape to showing early symptoms of deformation (Fig. 4h–n). At 48 h (Fig. 4o–u), the cytopathic effects were more prominent as cells appeared rounder, shrivelled, and indications of cell-to-cell contact were observed. By 72 h (Fig. 4v–z, aa, and ab), cells were substantially distorted with substantial disintegration of the monolayer, and some cells were dislodged from the surface of the

Table 3 Significant (χ^2 $P < 0.05$) positive and negative associations between virulence genes in *V. vulnificus*, *V. alginolyticus* and *Vibrio* spp

V. vulnificus	*apxIB*	*ompU*	*sodB*	*hlyB*	*fbpC*	*feoB*	*tldD*
viuB	χ^2: 1.466; OR 1.655 (0.728–3.760)	χ^2: 0.676; OR 1.343 (0.664–2.718)	χ^2: 1.159; OR 0.720 (0.656–0.790)	χ^2: 10.537[a]; OR 0.682 (0.612–0.759)	χ^2: 50.080[a]; OR 17.820 (6.992–45.414)	χ^2: 32.393[a]; OR 7.972 (3.695–17.202)	χ^2: 4.888[a]; OR 1.103 (1.043–1.165)
tldD	χ^2: 4.419[a]; OR 3.368 (1.027–11.051)	χ^2: 7.049[a]; OR 0.896 (0.841–0.953)	χ^2: 3.432; OR 7.455 (0.626–88.738)	χ^2: 8.762[a]; OR 5.526 (1.594–19.157)	χ^2: 2.068; OR 2.596 (0.678–9.930)	χ^2: 3.707; OR 4.121 (0.876–19.389)	
feoB	χ^2: 0.000; OR 1.004 (0.505–1.997)	χ^2: 0.006; OR 1.026 (0.552–1.907)	χ^2: 0.681; OR 0.375 (0.033–4.213)	χ^2: 2.244; OR 2.024 (0.794–5.158)	χ^2: 16.592[a]; OR 3.569 (1.914–6.655)		
fbpC	χ^2: 5.601[a]; OR 2.385 (1.148–4.952)	χ^2: 0.532; OR 1.260 (0.677–2.344)	χ^2: 6.517[a]; OR 3.608 (1.282–10.151)				
hlyB	χ^2: 1.106; OR 1.639 (0.649–4.142)	χ^2: 0.470; OR 0.721 (0.282–1.844)	χ^2: 7.399[a]; OR 13.909 (1.210–159.851)				
sodB	χ^2: 2.885; OR 6.333 (0.560–71.609)	χ^2: 1.305; OR 3.738 (0.332–42.055)	χ^2: 2.491; OR 0.543 (0.474–0.622)				
ompU	14.354[a]; OR 3.787 (1.861–7.705)						

V. alginolyticus	*asp*	*pvuA*	*tlh*
rtx	χ^2: 1.151; OR 1.250 (0.917–1.704)	χ^2: 2.143; OR 6.00 (0.478–75.344)	χ^2: 0.536, OR 1.111 (0.904–1.366)
tlh	χ^2: 6.964[a]; OR 0.071 (0.011–0.472)	χ^2: 0.938; OR 0.500 (0.296–0.844)	
pvuA	χ^2: 0.010; OR 1.167 (0.059–22.937)		

Vibrio spp.	*apxIB*	*ompU*	*sodB*	*hlyB*	*fbpC*	*feoB*	*tldD*
viuB	ND	χ^2: 3.733; OR 0.2 (0.035–1.154)	ND	ND	χ^2: 1.556; OR 0.333 (0.10–1.034)	χ^2: 3.733; OR 0.053 (0.606–14.864)	ND
tldD	ND	ND	ND	ND	ND	ND	
feoB	ND	χ^2: 0.630; OR 4.000 (0.117–136.957)	ND	ND	χ^2: 2.917; OR 0.167 (0.28–0.997)		
fbpC	ND	χ^2:0.467; OR 0.8 (0.516–1.240)	ND	ND			
hlyB	ND	ND	ND				
sodB	ND	ND					
o mpU	ND						

[a] Positive association at $p < 0.05$, χ^2-chi-square value, OR-odds ratio with 95% confidence interval, ND-not determined.

wells, exhibiting serious cellular damage and cell death. The progressive morphological alterations from spindle-shaped (HEK293) and epithelial-shaped (HepG2) to rounded, shrivelled, and deformed, alongside the gradual degradation of the cellular monolayer, underscore the cytopathic effects of *V. vulnificus* strains on both HEK293 and HepG2 cells over a 72-h period.

Uninfected HEK293 and HepG2 cells are demonstrated throughout the 72-h period, exhibiting the development of cells. During the initial 24 h of incubation (Fig. 3g), the HEK293 cell culture demonstrated spheroid and spindle growth patterns. At 48 h (Fig. 3n), most cells adopted a spindle-shaped adherence, followed by the formation of a dense cell layer over the 72-h incubation period (Fig. 3u). Throughout the 72-h incubation period (Fig. 3u), the HEK293 cells remained adhere to the surface of the wells in the plate displaying no changes in morphology or any stress-related detachment. As demonstrated in Fig. 4g, post-24-h incubation, HepG2 cells are epithelial in nature and maintain their polygonal form throughout the 72-h incubation period. During the 48-h incubation period (Fig. 4n), HepG2 cells exhibited distinct boundaries and established cell-to-cell contact; by the 72-h incubation period (Fig. 4u), HepG2 cells formed compact clusters. Like the HEK293 cells, the uninfected HepG2 cells maintained their epithelial morphology, exhibiting no indications of rounding, detachment, or damage during the 72-h incubation period. Over the 72-h timeframe, both HEK293 and HepG2 cells retained their unmodified shape as well as established increasing cell concentrations. No sign of contamination was detected during the experiment, confirming that external variables did not affect the results and maintaining the baseline viability and integrity of the assay.

3.5 Cell viability assay

The cell viability of HEK293 and HepG2 cells (Fig. 5a and b) was assessed over 24-, 48-, and 72-h following exposure to five *Vibrio vulnificus* isolates (V.v.137, V.v.406, V.v.419, V.v.420 and V.v.444), with comparisons made to *V. vulnificus* ATCC 27562 (positive control) and uninfected cells (negative control). Following 24-h incubation, HEK293 cells infected with isolate V.v.420 exhibited the lowest cell viability (15.53% ± 0.26) while those infected with V.v.137 showed the highest (77.34% ± 2.2). By 48 h, cell viability had notably decreased for all isolates exposed to V.v. 420, reducing to 1.01% ± 0.16 and V.v. 137 to 47.44% ± 2.2. By 72 h, the cell viability continued to decline, with HEK293 cells infected with V.v.406, V.v.419, and V.v.420 showing cell viabilities close to or below 1% compared to those exposed to V.v.137, which exhibited the highest cell viability of 12.07% ± 0.5. HEK293 cells treated with *V. vulnificus* ATCC 27562 (positive control) also showed a marked decrease in cell viability over time, from 58.44% ± 1.63 at 24 h to 1.70% ± 0.15 at 72 h whereas the negative control maintained near-complete cell viability across all time points (from 99.99% to 99.88%). HepG2 infected with V.v.419 demonstrated the lowest cell viability at 24 h (7.7% ± 0.89) as compared to V.v.137 (87% ± 1.03). By 48 hours, cell viability decreases markedly with cells exposed to V.v.419 reducing to 2.18% ± 0.2 and V.v.137 to 51.89% ± 0.65. By 72 h, substantial reduction in cell viability was observed with V.v.137 infected HepG2 cells decreasing to 7.25% ± 0.22, while cells infected with V.v.406, V.v.419, and V.v.420 displayed minimal viability levels below 2%. HEPG2 cells treated with the positive control followed a similar trend, reducing from 66.73 ± 2.23% at 24 h to 3.43 ± 0.73% by 72 h. The negative control consistently showed no notable reduction in cell viability (99.99% to 99.88%) throughout the assay. Analysis of variance (ANOVA) revealed significant differences among all samples in comparison to the negative control ($P \leq 0.0001$). However, no significant difference was detected between V.v.419 and V.v.420 at the 48-h incubation period for HEK293 and HepG2 cells, as well as among V.v.406, V.v.419, and V.v.420 at the 72-h incubation period for HEK293, and between V.v.406 and V.v.444 for HepG2. Furthermore, dose-response experiments, using serial dilutions of *V. vulnificus* suspensions demonstrated a proportional decrease in cell viability, supporting the role of virulence factors in cytotoxicity (Fig. S1–S6†).

4. Discussion

This study investigates the virulence gene profiling and cytotoxicity of *Vibrio* spp. isolated from treated wastewater effluent and receiving surface waters in South Africa, as inadequate wastewater management results in the contamination of environmental water sources and the proliferation of waterborne diseases.[33] The predominant pathogenic species, including *Vibrio cholerae*, *Vibrio parahaemolyticus*, *Vibrio vulnificus*, and *Vibrio alginolyticus*, are implicated in human infections associated with contaminated aquatic habitats and seafood.[34]

The PCR amplification of virulence genes in *V. vulnificus* and *V. alginolyticus* isolates elucidated the presence and distribution of essential virulence components. Of the eight virulence genes examined (*apxIB*, *ompU*, *sodB*, *hlyB*, *fbpC*, *viuB*, *tldD*, and *feoB*) in *V. vulnificus* (Fig. 1a and b), *viuB*, *fbpC*, and *feoB* were identified as the most frequent, indicating a significant frequency of these genes within the *V. vulnificus* population. Table 2 indicates that the virulence gene, *viuB*, was found in 72.47% ($n = 129$) of cases. *viuB* encodes vulnibactin, a siderophore that facilitates iron uptake in *V. vulnificus*.[10] *viuB* was detected in all clinical and environmental *V. vulnificus* isolates documented in a prior investigation.[35] Virulence genes *fbpC* and *feoB* were identified in 55.06% ($n = 98$) and 56.74% ($n = 101$) of isolates, respectively. These genes encode ferric (*fbpC*) and ferrous (*feoB*) iron transport systems, which are essential for *Vibrio* spp. survival as iron plays a crucial role in bacterial metabolism and gene regulation.[36] The occurrence of *ompU* in 35.39% ($n = 63$), *apxIB* in 24.72% ($n = 44$), and *hlyB* in 13.48% ($n = 24$) of isolates demonstrates a heterogeneous distribution of these virulence genes. Outer membrane protein U (*ompU*) is a conserved main outer membrane protein, which is extensively prevalent in pathogenic *Vibrio* spp.[37] This protein is identified as a significant adhesin in *V. cholerae* and *V. vulnificus*. Although the *apxIB* gene has been documented in *Actinobacillus pleuropneumoniae*, our results also identified the *apxIB* gene in *V. vulnificus* isolates.[38] It is crucial to mention that the primer employed for

this detection was created based on the genomic information collected from the *Vibrio vulnificus* ATCC 27562. The hemolysin region has been found to be highly conserved[39] with studies reporting *hlyB* exclusively in *V. cholera*[40–42] however in contrast with previous studies, this study reported *hlyB* in some *V. vulnificus* isolates. Conversely, *tldD* was identified in merely 6.74% ($n = 12$) of isolates, while *sodB* was detected in only 1.69% ($n = 3$) of isolates, indicating a diminished prevalence of these genes among the examined *V. vulnificus* isolates. A prior study, similarly, indicated the low incidence of *tldD* in another *Vibrio* spp.[43] For example, *V. anguillarum*, the *sodB* gene, which encodes superoxide dismutase (SOD), is essential for oxidative stress tolerance in *Vibrio vulnificus*. The low incidence of *sodB* contrasted with the previous findings where sewage exposure elevated the transcription of *sodB* in *Vibrio* isolates.[44]

Virulence gene detection in *V. alginolyticus* isolates ($n = 15$) (Fig. 2) revealed *rtxA*, encoding for a holotoxin[45] was the most prevalent, detected in 66.67% ($n = 10$) of isolates followed by *pvuA* which was detected in 46.67% ($n = 7$) of isolates. The prevalence of *pvuA* in this study was higher than *V. alginolyticus* isolated from seafood samples in Mexico city which reported 17.9% ($n = 285$).[46] A low prevalence of *asp* (13.33%, $n = 2$) and *tlh* (6.67%, $n = 1$) was observed in the *V. alginolyticus* isolates. These genes, *asp* (encodes for alkaline serine protease) and *tlh* (encodes for thermolabile hemolysins), are typically identified in *V. alginolyticus* isolated from seafood products[47] and were previously detected in silver sea bream (*Sparus sarba*) erythrocytes.[48] Overall, this analysis underscores the diversity in the distribution of virulence genes among *V. vulnificus* and *V. alginolyticus* isolates, providing valuable information for understanding the pathogenicity and virulence potential of these bacteria. Furthermore, the co-existence of two or more virulence genes in an isolate suggests that a subset of strains can exhibit multiple virulence factors simultaneously (Table S1†). Moderate to high multi-virulence gene index (MVGI) displayed among some strains reflects distinct virulence gene compositions highlighting pathogenic risks of these species especially in immunocompromised individuals.[24,49] Further investigation is warranted into how these virulence factors interact.

As observed in Table 3, descriptive analysis of crosstabs for virulence genes in *V. vulnificus* using Chi-squared analysis highlighted significant associations between these virulence factors and their contribution to the bacteria's pathogenicity. *feoB* and *fbpC* are both iron-transport related genes that showed significant association with each other indicating that iron acquisition is an important strategy contributing to the virulence of *V. vulnificus*.[50] The association between the vulnibactin encoding gene, *viuB*, and *hlyB*, *fbpC*, *feoB*, and *tldD* suggests the relationship between iron acquisition systems, iron transport and hemolysins provide a source of iron for these bacterial strains through lysis of the red blood cells contributing to the survival and pathogenicity of *V. vulnificus* in iron-limited environments.[51,52] The metalloprotease encoding gene, *tldD*, which is known to degrade host proteins and facilitate tissue invasion, was found to be associated with *apxIB*, *ompU*, and hlyB.[53] The association between *tldD* and *ompU* implies these adhesion and invasion mechanisms work together to enhance bacterial pathogenicity as well as a suggested coordinated response that results in cell lysis, through hemolysin activity, and tissue invasion.[54,55] The *apxIB* encodes for a transport protein that is involved with the transport of the RTX toxin leading to haemolytic and cytotoxic effects.[56] Significant association between *tldD* and *apxIB* suggests that once the metalloproteases have degraded the host's proteins such as the extracellular matrix components, it will allow *apxIB* to transport the RTX toxins to access and cause greater damage in the host tissues.[57,58] Additionally, the association between *fbpC* and *sodB* reflect a dual strategy in the bacterium's survival in hostile environments as

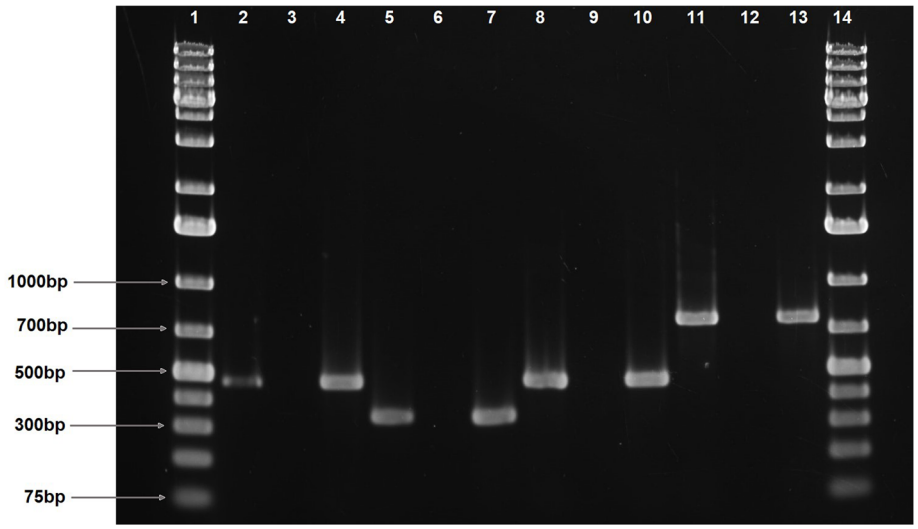

Fig. 2 PCR amplification of virulence genes identified in *V. alginolyticus*. Lanes 1 and 14, 1kb molecular marker; lanes 2, 4 shows *asp* (475bp) in the positive control and positive strain, respectively; lane 3, negative control; lanes 5 and 7, *pvuA* (343bp) in the positive control and positive strain, respectively; lane 6, negative control; lanes 8 and 10, *rtx* (473bp) in the positive control and positive strain, respectively; lane 9, negative control; lanes 11 and 13, *tlh* (770bp) in the positive control and positive strain, respectively; lane 12, negative control.

not only does it scavenge iron to promote growth but also enhances its defence against oxidative stress.[36,59] Despite a lower frequency of *asp* and *tlh* detected in *V. alginolyticus*, Table 3 showed a significant association was observed between these genes suggesting they play a coordinated role in the pathogenicity of the bacterium as the alkaline serine protease and thermolabile hemolysin assist with tissue degradation and breaking down of the host cell membranes, respectively.[60] Despite their low prevalence, the co-occurrence of these virulence genes could enhance the bacterium's ability to establish infection by potentially facilitating acquisition and immune evasion. The significant association between these virulence genes highlight the multifaceted nature of bacterial pathogenicity which contribute to the bacterium's survival, proliferation and invasion within a host.[61] Understanding the genetic associations between virulence factors in *V. vulnificus*, *V. alginolyticus* and another *Vibrio* spp. may help predict their pathogenic potential resulting in the development of targeted treatments or preventative measures, particularly for immunocompromised individuals who are vulnerable to severe infections.[62]

The odds ratio (OR) analysis presented in Table 3 elucidates potential correlations among several virulence genes within the examined bacterial strains that may enhance their pathogenicity.[32] In *V. vulnificus*, the high odds ratio between ratios between *viuB* and *fbpC* (OR 17.820, CI: 6.992–45.414) and *viuB* and *feoB* (OR 7.972, CI: 3.695–17.202) suggests the presence of these gene pairs may synergistically enhance pathogenicity in the bacterial strains even though broad confidence intervals suggest variability in the data that may be influenced by sample size or other factors requiring further validation in larger studies.[63] The odds ratio indicated that the associations between *ompU* and *apxIB* (OR 3.787, CI: 1.861–7.705), *fbpC* and *apxIB* (OR 2.385, CI: 1.148–4.952), and *fbpC* and *sodB* (OR 3.608, CI: 1.282–10.151) were more robust, as their confidence intervals do not encompass one, suggesting functional links between these genes that may enhance virulence.[32,64] In contrast, minimal association was observed between *rtx* and *asp* (OR 1.250, CI: 0.917–1.704) in *V. alginolyticus* and *feoB* and *apxIB* (OR 1.004, CI: 0.505–1.997) in *V. vulnificus* as the odds ratios were close to one and confidence intervals overlapped one suggesting that these gene pairs do not contribute to increased virulence.[63] In *Vibrio* spp., the odds ratios were approximately one or lower, accompanied by wide confidence intervals, indicating no significant associations between the gene pairs. However, due to the limited sample size of these bacterial strains, further research with a larger dataset is necessary to elucidate the relationship between the gene pairs in these isolates.[65]

V. vulnificus, a bacterium present in warm coastal waters, represents a considerable risk to human health, especially for those with liver illness or immunocompromised conditions.[30,66] It may lead to severe sepsis and necrotizing infections with fatality rates of 50%.[30] In this work, exposure to *V. vulnificus* resulted in severe cytotoxic effects on HEK293 and HepG2 cell lines, defined by morphological alterations and decreased cell viability, underlining the pathogen's potential clinical significance. *V. vulnificus* also elicits robust inflammatory responses, resulting in cellular damage and death.[67,68] The cytotoxicity observed at a selected concentration of 10^8 CFU mL^{-1}, while higher than average environmental levels, provides important insights into potential health risks during peak exposure scenarios. The dose-response experiments (Fig. S1–S6†) confirmed that cytotoxic effects occur proportionally even at lower concentrations, indicating that environmental *Vibrio* strains may pose health risks under real-world conditions, particularly for immunocompromised individuals.[12,69–72] These findings suggest that *Vibrio* strains present in wastewater, even at concentrations lower than those used in this study, may pose significant health risks, especially through recreational water activities or consumption of seafood from contaminated waters. The rounding and detachment of HEK293 cells (Fig. 3) and the shrinkage and detachment of HepG2 cells (Fig. 4), transitioning from spindle- and epithelial-shaped forms, indicate that the cytotoxic effects are not confined to a single cell type but impact multiple cellular targets. This extensive cytotoxicity corresponds with prior research emphasizing the virulent characteristics of *V. vulnificus* in host tissues.[73] The disparate reactions noted between HEK293 and HepG2 cells, with a more significant cytotoxic effect in HEK293 cells, may be ascribed to intrinsic variations in cellular pathways and vulnerabilities. HEK293 cells, generated from human embryonic kidney cells, and HepG2 cells, derived from human liver carcinoma cells, feature unique metabolic and signalling pathways, which may influence their response to bacterial toxins and virulence factors. Additional examination of these cellular pathways may yield profound insights into the precise connections between *V. vulnificus* and other cell types.

Renal impairment elevates the probability of *V. vulnificus* infection, highlighting the necessity of comprehending its cytotoxic consequence.[74] This study revealed *V. vulnificus*'s capacity to lethally affect HEK293 cells, signifying its potential to harm renal tissue. While *V. vulnificus* infections are mostly linked to gastrointestinal disorders, they may also result in systemic infections and consequences, such as renal failure.[75] Chronic conditions such as liver disease and hemochromatosis elevate the likelihood of *V. vulnificus* infections.[76] Iron is crucial for bacterial physiological functions, including transcription, DNA replication, metabolic activities, and energy production through respiration. Consequently, many pathogenic bacteria, such as *V. vulnificus*, have evolved siderophores and iron acquisition mechanisms to extract iron from their hosts.[77] Kidney and liver cells necessitate iron for metabolic functions, with the liver significantly coordinating iron homeostasis by storing, using intracellularly, or mobilizing it for systemic distribution.[78,79] HepG2 and HEK293 cells, being abundant in iron due to their origin from human liver and kidney tissue, respectively, serve as optimal targets for bacterial iron acquisition systems. As previously stated, *viuB* encodes the siderophore vulnibactin, which sequesters iron from the host, hence altering cellular processes and enhancing cytotoxicity through hepatocyte damage.[80] The ferric and ferrous iron transport systems encoded by *fbpC* and *feoB*, respectively, augment the capacity of *V. vulnificus* to assimilate iron, leading to oxidative stress and ultimately host cell mortality.[81] Reactive oxygen species (ROS) are generated as part of the host's immunological response to

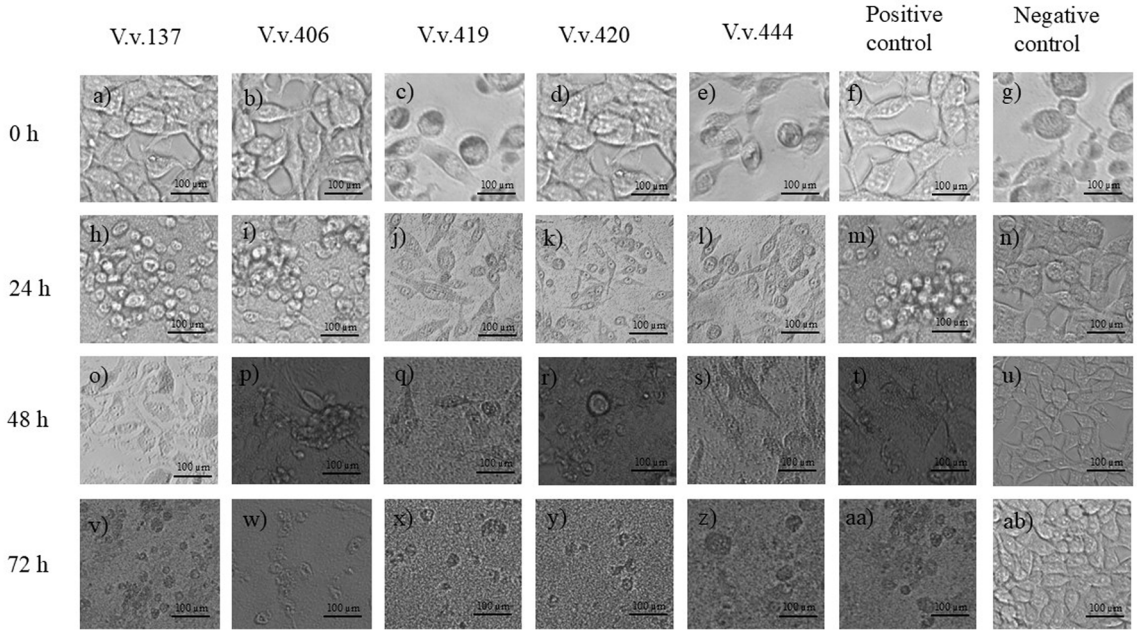

Fig. 3 Cytopathic effects of *Vibrio vulnificus* (V.v.) isolates on HEK293 cells over a 72 h period. Images (a–g) correspond to isolates V.v.137, V.v.406, V.v.419, V.v.420, V.v.444, positive control, and negative control, respectively, at 0 h. Images (h–n) display the same conditions at 24 h, images (o–u) at 48 h and images (v–ab) at 72 h.

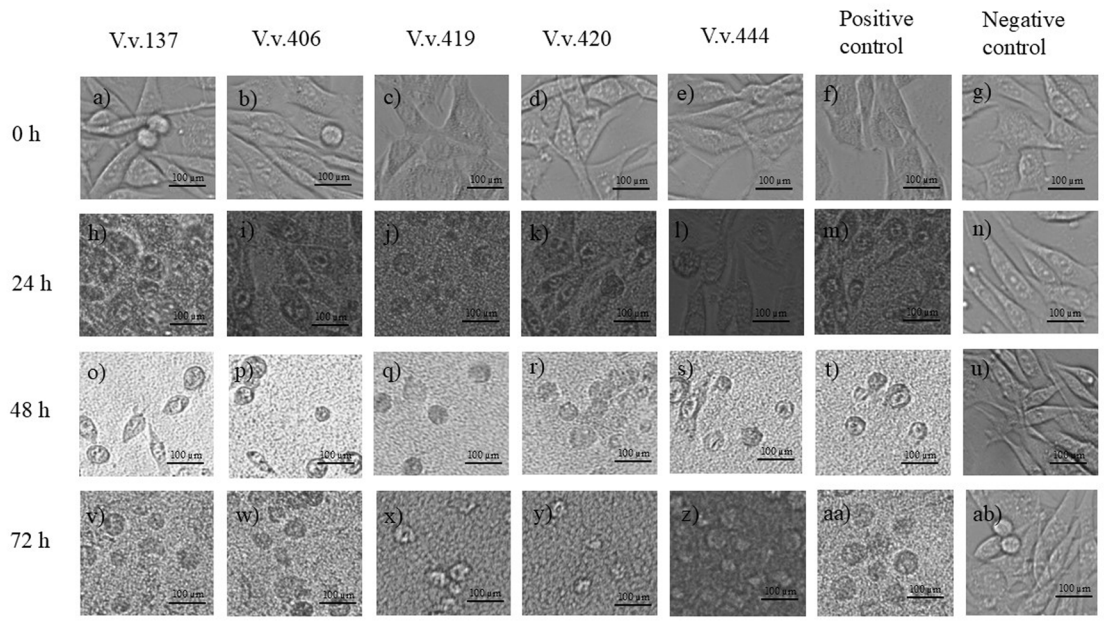

Fig. 4 Cytopathic effects of *Vibrio vulnificus* (V.v.) isolates on HepG2 cells over a 72 h period. Images (a–g) show the effects of isolates V.v.137, V.v.406, V.v.419, V.v.420, V.v.444, positive control, and negative control, respectively, at 0 h. Images (h–n) represent the same conditions at 24 h, images (o–u) at 48 h and images (v–ab) at 72 h.

infections; however, bacteria employ enzymes like superoxide dismutase to mitigate this response.[82] The generation of ROS may elicit an immunological response in HepG2 and HEK293 cells against bacterial infection; however, *sodB* produces superoxide dismutase (SOD), which may facilitate the survival of *V. vulnificus*, resulting in prolonged infection and harmful effects.[83] The hemolysins encoded by *hlyB* may create pores in the membranes of HepG2 and HEK293 cells, compromising membrane integrity and leading to cell lysis, while the outer membrane protein encoded by *ompU* may facilitate the adhesion of *V. vulnificus* to HepG2 and HEK293 cells, thereby augmenting the bacteria's capacity to colonize host tissues.[37,84] The

metalloproteases produced by *tldD* may be responsible for the breakdown of essential cellular proteins, including structural components or immunological proteins, in HepG2 and HEK293 increasing cytotoxicity.[43] Finally, the inclusion of *apxIB* enhances the cytotoxicity of the *Vibrio* isolates, as the RTX-I toxin it carries creates gaps in the host cell membranes, leading to cell lysis and apoptosis.[85] This will cause cellular damage and reduce cell viability, as illustrated in Fig. 5, hence enhancing the virulence of these bacterial strains. Additionally, analysis of variance (ANOVA) revealed significant differences among all samples compared to the negative control ($P \leq 0.0001$), indicating that infection with the *Vibrio vulnificus* strains impacted cell viability.

These findings have significant public health implications for regions where *V. vulnificus* is endemic in coastal and estuarine waters. Enhanced surveillance of water quality parameters and pathogen monitoring in high-risk areas is essential, particularly during warmer months when *Vibrio* populations typically increase. Public health authorities should prioritize targeted education campaigns for vulnerable populations, including immunocompromised individuals and those with chronic liver disease, regarding risks associated with exposure to potentially contaminated waters. The identification of key virulence determinants also provides molecular targets for developing novel therapeutic interventions, particularly protease and haemolysing inhibitors that could supplement current antibiotic treatments. This study provides important insights into the virulence gene profiles and cytotoxic potential of environmental *Vibrio* spp. isolates, though several limitations warrant consideration. Our analysis focused primarily on gene presence and *in vitro* cytotoxicity assessments, which establish a foundation for understanding pathogenic potential but do not fully elucidate the functional mechanisms of virulence factor expression or host–pathogen interactions. Future investigations incorporating functional assays for haemolytic activity, inflammatory cytokine induction, and iron acquisition mechanisms will be necessary to comprehensively characterize the pathogenic mechanisms of these environmental isolates.

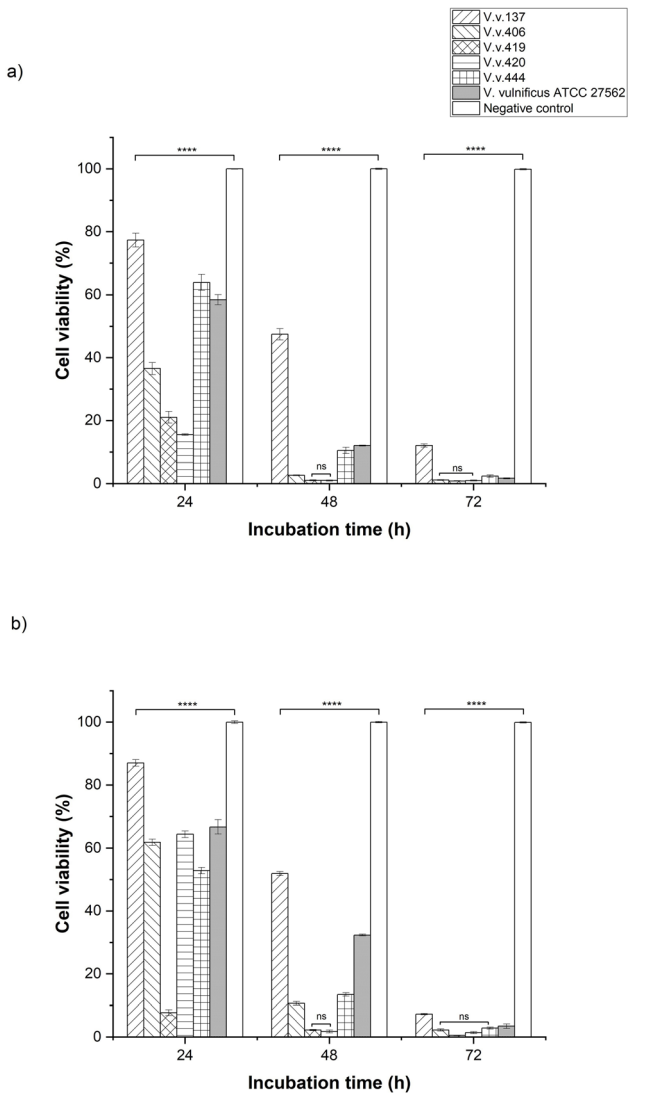

Fig. 5 Viability testing of HEK293 (a) and HepG2 (b) cells treated with V.v.137, V.v.406, V.v.419, V.v.420 and V.v.444 and the positive (*V. vulnificus* ATCC 27562) and negative control after incubated for 24, 48 and 72 h. **** indicates significant difference at $p \leq 0.0001$.

5. Conclusion

Based on virulence gene profiling and cytotoxic data, this work examined the pathogenicity of 200 *Vibrio* isolates from treated wastewater effluent and receiving surface waters of four wastewater treatment plants in Durban, KwaZulu-Natal. In *V. vulnificus* isolates ($n = 178$), the most frequently detected virulence gene was *viuB*, followed by *feoB*, *fbpC*, *ompU*, *apxIB*, *hlyB*, *tldD*, and *sodB* whereas highest virulence gene detection rates were observed for *rtx*, followed *pvuA*, *asp* and *tlh* in *V. alginolyticus* ($n = 15$). In the *Vibrio* spp. ($n = 7$), the most common virulence gene detected was *viuB*, followed by *ompU*, *feoB* and *fbpC*. Significant associations between virulence genes were identified in *V. vulnificus* such as between *viuB* and *fbpC*, *feoB* and *fbpC*, and *hlyB* and *sodB* whereas in *V. alginolyticus*, significant association were observed between *tlh* and *asp* emphasizing the interactions and robust relationships among virulence genes. Infection of HEK293 and HepG2 cells with five selected *V. vulnificus* strains, V.v.137, V.v.406, V.v.419, V.v.420 and V.v.444, highlighted the pathogenic potential of these isolates. HEK293 and HepG2 exhibited morphological changes including, detachment, shrinkage and cell death following infection with all five *V. vulnificus* isolates. Additionally, exposure of these cells to V.v.419 and V.v.420 resulted in rapid declines in cell viability falling below 2% within 72 h, indicating severe cytotoxic effects. In contrast, less virulent strains like V.v.137 enabled HEK293 and HepG2 cells to retain higher cell viability despite demonstrating a progressive decline over time. These findings highlight the prevalence and diversity of virulence genes among *Vibrio* spp. isolated from wastewater and environmental waters, their significant associations, and their marked cytotoxic effects on human cell lines. The study underlines the importance of constant monitoring and enhancement of wastewater treatment processes to ensure successful elimination of pathogenic

bacteria. Furthermore, public health programs should raise awareness about the dangers of exposure to contaminated water sources as well as promoting safe practices for recreational water use and seafood intake.

Ethical approval

This research did not contain any studies involving animal or human participants, nor did it take place on any private or protected areas. No specific permissions were required for corresponding locations.

Consent to participate

All the authors are aware and agree to participating in this manuscript.

Consent to publish

All the authors agree to publish this manuscript.

Data availability

Data are contained within the article or ESI Material.†

Author contributions

Conceptualization, K. R. and A. O.·O.; methodology, K. R. and A. O.·O.; validation, K. R. and A. O.·O.; formal analysis, K. R.; investigation, K. R. and A. O.·O.; resources, A. O.·O.; data curation, K. R.; writing K. R. and A. O.·O.; visualization, K. R.; supervision, A. O.·O.; project administration, A. O.·O.; funding acquisition, K. R. A. O. O. All authors have read and agreed to the published version of the manuscript.

Conflicts of interest

The authors declare no conflicts of interest.

Acknowledgements

National Research Foundation of South Africa (NRF grant no. UID 118324 and 139095). We appreciate the eThekwini Municipality for granting us permission to collect samples from the wastewater treatments plants in the Durban area, KwaZulu-Natal, South Africa.

References

1 A. Murei, I. Kamika, A. Samie and M. N. B. Momba, Assessment of the water sources for potential channels of faecal contamination within Vhembe District Municipality using sanitary inspections and hydrogen sulphide test, *Sci. Rep.*, 2023, **13**(1), 1–13, DOI: **10.1038/s41598-023-33551-y**.

2 O. Osuolale and A. Okoh, Assessment of the physicochemical qualities and prevalence of *Escherichia coli* and *Vibrios* in the final effluents of two wastewater treatment plants in South Africa: Ecological and public health implications, *Int. J. Environ. Res. Public Health*, 2015, **12**(10), 13399–13412, DOI: **10.3390/ijerph121013399**.

3 P. Verlicchi and V. Grillini, Surface water and groundwater quality in South Africa and Mozambique—analysis of the most critical pollutants for drinking purposes and challenges in water treatment selection, *Water*, 2020, **12**(1), 305, DOI: **10.3390/W12010305**.

4 I. George, P. Crop and P. Servais, Fecal coliform removal in wastewater treatment plants studied by plate counts and enzymatic methods, *Water Res.*, 2002, **36**(10), 2607–2617, DOI: **10.1016/S0043-1354(01)00475-4**.

5 C. O. Osunmakinde, R. Selvarajan, B. B. Mamba and T. A. M. Msagati, Profiling bacterial diversity and potential pathogens in wastewater treatment plants using high-throughput sequencing analysis, *Microorganisms*, 2019, **7**(11), 506, DOI: **10.3390/MICROORGANISMS7110506**.

6 O. Osuolale and A. Okoh, Isolation and antibiotic profile of *Vibrio* spp. in final effluents of two wastewater treatment plants in the Eastern Cape of South Africa, *bioRxiv*, 2018330456, DOI: **10.1101/330456**.

7 K. Zhou, K. Y. Tian, X. Q. Liu, *et al.*, Characteristic and otopathogenic analysis of a *Vibrio alginolyticus* strain responsible for chronic otitis externa in China, *Front. Microbiol.*, 2021, **12**, 750642, DOI: **10.3389/FMICB.2021.750642/FULL**.

8 A. Sampaio, V. Silva, P. Poeta and F. Aonofriesei, *Vibrio* spp.: life strategies, ecology, and risks in a changing environment, *Diversity*, 2022, **14**(2), 97, DOI: **10.3390/D14020097**.

9 World Health Organization/Department of Control of Neglected Tropical Diseases, *Weekly epidemiological record Relevé épidémiologique hebdomadaire. Weekly epidemiological record*, 2018, **http://www.who.int/wer2018,93,649-660No48%0Ahttp://www.who.int/wer**.

10 C. D'souza, K. S. Prithvisagar, V. K. Deekshit, I. Karunasagar, I. Karunasagar and B. K. Kumar, Exploring the pathogenic potential of *Vibrio vulnificus* isolated from seafood harvested along the Mangaluru Coast, India, *Microorganisms*, 2020, **8**(7), 1–15, DOI: **10.3390/MICROORGANISMS8070999**.

11 W. A. Norfolk, C. Shue, W. M. Henderson, D. A. Glinski and E. K. Lipp, *Vibrio alginolyticus* growth kinetics and the metabolic effects of iron, *Microbiol. Spectrum*, 2023, **11**(6), e02680, DOI: **10.1128/spectrum.02680-23**.

12 C. Baker-Austin, J. D. Oliver, M. Alam, *et al.*, *Vibrio* spp. infections, *Nat. Rev. Dis. Primers*, 2018, **4**(1), 1–19, DOI: **10.1038/s41572-018-0005-8**.

13 H. Byun, I. J. Jung, J. Chen, J. L. Valencia and J. Zhu, Siderophore piracy enhances *Vibrio cholerae* environmental survival and pathogenesis, *Microbiology*, 2020, **166**(11), 1038, DOI: **10.1099/MIC.0.000975**.

14 M. A. Echazarreta and K. E. Klose, *Vibrio* flagellar synthesis, *Front. Cell. Infect. Microbiol.*, 2019, **9**, 131, DOI: **10.3389/FCIMB.2019.00131**.

15 H. A. Ganie, A. Choudhary and S. Baranwal, Structure, regulation, and host interaction of outer membrane

protein U (OmpU) of *Vibrio* species, *Microb. Pathog.*, 2022, **162**, 105267, DOI: 10.1016/J.MICPATH.2021.105267.

16 H. Gao, J. Xu, X. Lu, *et al.*, Expression of hemolysin is regulated under the collective actions of HapR, Fur, and HlyU in *Vibrio cholerae* El Tor serogroup O1, *Front. Microbiol.*, 2018, **9**, 352724, DOI: 10.3389/FMICB.2018.01310/BIBTEX.

17 S. J. Krebs and R. K. Taylor, Protection and attachment of *Vibrio cholerae* mediated by the toxin-coregulated pilus in the infant mouse model, *J. Bacteriol.*, 2011, **193**(19), 5260, DOI: 10.1128/JB.00378-11.

18 M. Mavhungu, T. O. Digban and U. U. Nwodo, Incidence and virulence factor profiling of *Vibrio* species: a study on hospital and community wastewater effluents, *Microorganisms*, 2023, **11**(10), 2449, DOI: 10.3390/MICROORGANISMS11102449.

19 H. Moeinizadeh and M. Shaheli, Frequency of *hlyA, hlyB, hlyC* and *hlyD* genes in uropathogenic *Escherichia coli* isolated from UTI patients in Shiraz, *GMS Hyg. Infect. Control*, 2021, **16**, Doc25, DOI: 10.3205/DGKH000396.

20 N. Mohamad, M. N. A. Amal, M. Z. Saad, *et al.*, Virulence-associated genes and antibiotic resistance patterns of *Vibrio* spp. isolated from cultured marine fishes in Malaysia, *BMC Vet. Res.*, 2019, **15**(1), 1–13, DOI: 10.1186/S12917-019-1907-8/TABLES/4.

21 K. Schwartz, J. A. Hammerl, C. Göllner and E. Strauch, Environmental and clinical strains of *Vibrio cholerae* non-O1, non-O139 from Germany possess similar virulence gene profiles, *Front. Microbiol.*, 2019, **10**, 438958, DOI: 10.3389/FMICB.2019.00733/BIBTEX.

22 C. L. Tarr, J. S. Patel, N. D. Puhr, E. G. Sowers, C. A. Bopp and N. A. Strockbine, Identification of *Vibrio* isolates by a multiplex PCR assay and *rpoB* sequence determination, *J. Clin. Microbiol.*, 2007, **45**(1), 134–140, DOI: 10.1128/JCM.01544-06.

23 C. H. Liu, W. Cheng, J. P. Hsu and J. C. Chen, *Vibrio alginolyticus* infection in the white shrimp *Litopenaeus vannamei* confirmed by polymerase chain reaction and *16S rDNA* sequencing, *Dis. Aquat. Org.*, 2004, **61**(1–2), 169–174, DOI: 10.3354/dao061169.

24 O. E. Abioye, C. A. Osunla, N. Nontongana and A. I. Okoh, Occurrence of virulence determinants in *Vibrio cholerae, Vibrio mimicus, Vibrio alginolyticus*, and *Vibrio parahaemolyticus* isolates from important water resources of Eastern Cape, South Africa, *BMC Microbiol.*, 2023, **23**(1), 316, DOI: 10.1186/S12866-023-03060-Z.

25 J. Sahandi, P. Sorgeloos, L. Xiao, *et al.*, The use of selected bacteria and yeasts to control *Vibrio* spp. in live food, *Antibiotics*, 2019, **8**(3), 95, DOI: 10.3390/antibiotics8030095.

26 J. Sun, J. Zheng, G. Wang, Y. Li and H. Shen, Apoptotic effect of *Vibrio vulnificus* cytolysin on A549 human lung adenocarcinoma cells, *Mol. Med. Rep.*, 2012, **5**(3), 668–674, DOI: 10.3892/mmr.2011.690.

27 C. K. Constante, J. Rodríguez, S. Sonnenholzner and C. Domínguez-Borbor, Adaptation of the methyl thiazole tetrazolium (MTT) reduction assay to measure cell viability in *Vibrio* spp, *Aquaculture*, 2022, **560**, 738568, DOI: 10.1016/j.aquaculture.2022.738568.

28 W. Chao, Z. Zhe, L. Yupeng, *et al.*, Type III secretion 1 effector gene diversity among *Vibrio* isolates from coastal areas in China, *Front. Cell. Infect. Microbiol.*, 2020, **10**, 301, DOI: 10.3389/fcimb.2020.00301.

29 K. D. Brumfield, A. J. Chen, M. Gangwar, *et al.*, Environmental Factors Influencing Occurrence of *Vibrio parahaemolyticus* and *Vibrio vulnificus*, *Appl. Environ. Microbiol.*, 2023, **89**(6), e0030723, DOI: 10.1128/AEM.00307-23.

30 M. A. Horseman and S. Surani, A comprehensive review of *Vibrio vulnificus*: An important cause of severe sepsis and skin and soft-tissue infection, *Int. J. Infect. Dis.*, 2011, **15**(3), e157–e166, DOI: 10.1016/J.IJID.2010.11.003.

31 M. K. Jones and J. D. Oliver, *Vibrio vulnificus*: Disease and pathogenesis, *Infect. Immun.*, 2009, **77**(5), 1723–1733, DOI: 10.1128/IAI.01046-08.

32 M. Szumilas, Explaining Odds Ratios, *J. Can. Acad. Child Adolesc. Psychiatry*, 2010, **19**(3), 227, Accessed November 6, 2024, https://pmc.ncbi.nlm.nih.gov/articles/PMC2938757/.

33 B. J. Singh, A. Chakraborty and R. Sehgal, A systematic review of industrial wastewater management: Evaluating challenges and enablers, *J. Environ. Manage.*, 2023, **348**, 119230, DOI: 10.1016/J.JENVMAN.2023.119230.

34 A. Castello, V. Alio, S. Sciortino, *et al.*, Occurrence and molecular characterization of potentially pathogenic *Vibrio* spp. in seafood collected in Sicily, *Microorganisms*, 2022, **11**(1), 53, DOI: 10.3390/MICROORGANISMS11010053.

35 N. Yokochi, S. Tanaka, K. Matsumoto, *et al.*, Distribution of virulence markers among *Vibrio vulnificus* isolates of clinical and environmental origin and regional characteristics in Japan, *PLoS One*, 2013, **8**(1), e55219, DOI: 10.1371/JOURNAL.PONE.0055219.

36 A. Pramanik and R. K. Vibhuti, Molecular mechanism of iron transport systems in *Vibrio*, *J. Pure Appl. Microbiol.*, 2022, **16**(1), 116–129, DOI: 10.22207/JPAM.16.1.77.

37 X. Liu, H. Gao, N. Xiao, Y. Liu, J. Li and L. Li, Outer membrane protein U (OmpU) mediates adhesion of *Vibrio mimicus* to host cells via two novel n-terminal motifs, *PLoS One*, 2015, **10**(3), e0119026, DOI: 10.1371/journal.pone.0119026.

38 S. J. Foote, J. T. Bossé, A. B. Bouevitch, P. R. Langford, N. M. Young and J. H. E. Nash, The complete genome sequence of Actinobacillus pleuropneumoniae L20, *J. Bacteriol.*, 2008, **190**(4), 1495–1496, DOI: 10.1128/JB.01845-07.

39 J. L. Rock and D. R. Nelson, Identification and characterization of a hemolysin gene cluster in *Vibrio anguillarum*, *Infect. Immun.*, 2006, **74**(5), 2777–2786, DOI: 10.1128/IAI.74.5.2777-2786.2006/ASSET/79A6BEA6-02D4-4BF6-AFB6-93E6ACA67758/ASSETS/GRAPHIC/ZII0050658670006.JPEG.

40 R. A. Alm and P. A. Manning, Characterization of the *hlyB* gene and its role in the production of the El Tor haemolysin of *Vibrio cholerae* O1, *Mol. Microbiol.*, 1990, **4**(3), 413–425, DOI: 10.1111/J.1365-2958.1990.TB00608.X.

41 I. Altinoglu, G. Abriat, A. Carreaux, *et al.*, Analysis of HubP-dependent cell pole protein targeting in *Vibrio cholerae* uncovers novel motility regulators, *PLOS Genet.*, 2022, **18**(1), e1009991, DOI: 10.1371/journal.pgen.1009991.
42 M. A. Matilla and T. Krell, The effect of bacterial chemotaxis on host infection and pathogenicity, *FEMS Microbiol. Rev.*, 2018, **42**(1), 40–67, DOI: 10.1093/femsre/fux052.
43 I. Vasquez, T. Cao, S. Chakraborty, *et al.*, Comparative genomics analysis of *Vibrio anguillarum* isolated from lumpfish (Cyclopterus lumpus) in Newfoundland reveal novel chromosomal organizations, *Microorganisms*, 2020, **8**(11), 1666, DOI: 10.3390/microorganisms8111666.
44 J. W. Conrad and V. J. Harwood, Sewage Promotes *Vibrio vulnificus* growth and alters gene transcription in *Vibrio vulnificus* CMCP6, *Microbiol. Spectrum*, 2022, **10**(1), e0191321, DOI: 10.1128/spectrum.01913-21.
45 F. Håkonsholm, B. T. Lunestad, J. R. Aguirre Sánchez, J. Martinez-Urtaza, N. P. Marathe and C. S. Svanevik, *Vibrios* from the Norwegian marine environment: Characterization of associated antibiotic resistance and virulence genes, *Microbiologyopen*, 2020, **9**(9), 1–19, DOI: 10.1002/mbo3.1093.
46 A. K. Álvarez-Contreras, E. I. Quiñones-Ramírez and C. Vázquez-Salinas, Prevalence, detection of virulence genes and antimicrobial susceptibility of pathogen *Vibrio* species isolated from different types of seafood samples at "La Nueva Viga" market in Mexico City, *Antonie van Leeuwenhoek*, 2021, **114**(9), 1417–1429, DOI: 10.1007/S10482-021-01591-X.
47 H. Rui, Q. Liu, Y. Ma, Q. Wang and Y. Zhang, Roles of LuxR in regulating extracellular alkaline serine protease A, extracellular polysaccharide and mobility of *Vibrio alginolyticus*, *FEMS Microbiol. Lett.*, 2008, **285**(2), 155–162, DOI: 10.1111/J.1574-6968.2008.01185.X.
48 S. K. Wong, X. H. Zhang and N. Y. S. Woo, *Vibrio alginolyticus* thermolabile hemolysin (TLH) induces apoptosis, membrane vesiculation and necrosis in sea bream erythrocytes, *Aquaculture*, 2012, **330–333**, 29–36, DOI: 10.1016/j.aquaculture.2011.12.012.
49 M. Restrepo-Benavides, D. Lozano-Arce, L. N. Gonzalez-Garcia, *et al.*, Unveiling potential virulence determinants in *Vibrio* isolates from *Anadara tuberculosa* through whole genome analyses, *Microbiol. Spectrum*, 2024, **12**(2), e0292823, DOI: 10.1128/SPECTRUM.02928-23/SUPPL_FILE/SPECTRUM.02928-23-S0006.XLSX.
50 K. Miyamoto, H. Kawano, N. Okai, *et al.*, Iron-utilization system in *Vibrio vulnificus* M2799, *Mar. Drugs*, 2021, **19**(12), 710, DOI: 10.3390/MD19120710.
51 C. Gómez-Garzón and S. M. Payne, Divide and conquer: genetics, mechanism, and evolution of the ferrous iron transporter Feo in Helicobacter pylori, *Front. Microbiol.*, 2023, **14**, 1219359, DOI: 10.3389/FMICB.2023.1219359/BIBTEX.
52 J. R. Sheldon, H. A. Laakso and D. E. Heinrichs, Iron acquisition strategies of bacterial pathogens, *Microbiol. Spectrum*, 2016, **4**(2), DOI: 10.1128/microbiolspec.VMBF-0010-2015.
53 X. Tang, Q. Yang, Z. Nan, T. Wang, Y. Li and Z. Wu, The potential compensatory mechanism between *pmbA* and *tldD* governing the virulence of *Aeromonas veronii* and its implications on the immune response in freshwater bivalve (*Hyriopsis cumingii*), *Aquaculture*, 2025, **595**, 741524, DOI: 10.1016/J.AQUACULTURE.2024.741524.
54 Z. Li, Y. Fan, Z. Li, *et al.*, Nonhemolysis of epidemic El Tor biotype strains of *Vibrio cholerae* is related to multiple functional deficiencies of hemolysin A, *Gut Pathog.*, 2019, **11**(1), 1–10, DOI: 10.1186/S13099-019-0316-7/TABLES/3.
55 D. Meparambu Prabhakaran, T. Ramamurthy and S. Thomas, Genetic and virulence characterisation of *Vibrio parahaemolyticus* isolated from Indian coast, *BMC Microbiol.*, 2020, **20**(1), 62, DOI: 10.1186/S12866-020-01746-2.
56 J. Liu, X. Chen, C. Tan, *et al.*, In vivo induced RTX toxin ApxIVA is essential for the full virulence of *Actinobacillus pleuropneumoniae*, *Vet. Microbiol.*, 2009, **137**(3–4), 282–289, DOI: 10.1016/J.VETMIC.2009.01.011.
57 K. Dzobo and C. Dandara, The extracellular matrix: Its composition, function, remodeling, and role in tumorigenesis, *Biomimetics*, 2023, **8**(2), 146, DOI: 10.3390/BIOMIMETICS8020146.
58 M. Kamali, M. Carossino, F. Del Piero, *et al.*, Pathological features and genomic characterization of an *Actinobacillus equuli* subsp. *equuli* bearing unique virulence-associated genes from an adult horse with pleuropneumonia, *Pathogens*, 2023, **12**(2), 224, DOI: 10.3390/PATHOGENS12020224/S1.
59 H. Najmuldeen, R. Alghamdi, F. Alghofaili and H. Yesilkaya, Functional assessment of microbial superoxide dismutase isozymes suggests a differential role for each isozyme, *Free Radical Biol. Med.*, 2019, **134**, 215–228, DOI: 10.1016/J.FREERADBIOMED.2019.01.018.
60 B. Yang, S. Zhai, X. Li, *et al.*, Identification of *Vibrio alginolyticus* as a causative pathogen associated with mass summer mortality of the Pacific Oyster (*Crassostrea gigas*) in China, *Aquaculture*, 2021, **535**, 736363, DOI: 10.1016/J.AQUACULTURE.2021.736363.
61 J. Soni, S. Sinha and R. Pandey, Understanding bacterial pathogenicity: a closer look at the journey of harmful microbes, *Front. Microbiol.*, 2024, **15**, 1370818, DOI: 10.3389/FMICB.2024.1370818.
62 G. Muteeb, M. T. Rehman, M. Shahwan and M. Aatif, Origin of antibiotics and antibiotic resistance, and their impacts on drug development: a narrative review, *Pharmaceuticals*, 2023, **16**(11), 1615, DOI: 10.3390/PH16111615.
63 S. Tenny and M. R. Hoffman, Odds Ratio, *Encycl. Genet. Genomics Proteomics Inform.*, 2023, 1388, DOI: 10.1007/978-1-4020-6754-9_11771.
64 N. G. Djomgoue, L. J. Fonbah, A. I. Mbulli, K. Ousenu and T. C. Bonglavnyuy, Risk factors and associated outcomes of virulence genes *eae, entB*, and *pipD* Carriage in *Escherichia coli, Klebsiella pneumoniae*, and *Salmonella* spp. from HIV-1 and HIV-negative gastroenteritis patients in the Dschang Regional Hospital Annex, *Cureus*, 2023, **15**(7), e42329, DOI: 10.7759/CUREUS.42329.

65 S. Nemes, J. M. Jonasson, A. Genell and G. Steineck, Bias in odds ratios by logistic regression modelling and sample size, *BMC Med. Res. Methodol.*, 2009, **9**(1), 1–5, DOI: 10.1186/1471-2288-9-56/FIGURES/3.

66 K. E. Phillips and K. J. F. Satchell, Vibrio vulnificus: From oyster colonist to human pathogen, *PLOS Pathog.*, 2017, **13**(1), e1006053, DOI: 10.1371/JOURNAL.PPAT.1006053.

67 K. B. Kwon, J. Y. Yang, D. G. Ryu, *et al.*, *Vibrio vulnificus* cytolysin induces superoxide anion-initiated apoptotic signaling pathway in human ECV304 cells, *J. Biol. Chem.*, 2001, **276**(50), 47518–47523, DOI: 10.1074/JBC.M108645200.

68 C. Murciano, L. I. Hor and C. Amaro, Host-pathogen interactions in *Vibrio vulnificus*: responses of monocytes and vascular endothelial cells to live bacteria, *Future Microbiol.*, 2015, **10**(4), 471–487, DOI: 10.2217/FMB.14.136.

69 J. M. Pérez Martín, P. Fernández Freire, A. Peropadre and M. J. Hazen, Cytotoxic evaluation of a mixture of eight pollutants at environmental relevant concentrations, *Rev. Toxicol.*, 2014, **31**(2), 172–175.

70 C. Kataoka and S. Kashiwada, Ecological risks due to immunotoxicological effects on aquatic organisms, *Int. J. Mol. Sci.*, 2021, **22**(15), 8305, DOI: 10.3390/ijms22158305.

71 C. Viegas, P. Pena, B. Gomes, M. Dias, L. A. Caetano and S. Viegas, Are in vitro cytotoxicity assessments of environmental samples useful for characterizing the risk of exposure to multiple contaminants at the workplace? A systematic review, *Toxics*, 2022, **10**(2), 72, DOI: 10.3390/toxics10020072.

72 J. D. Oliver, The biology of *Vibrio vulnificus*, *Microbiol. Spectrum*, 2015, **3**(3), 0001–2014, DOI: 10.1128/microbiolspec.VE-0001-2014.

73 Y. R. Kim, S. E. Lee, H. Kook, *et al.*, *Vibrio vulnificus* RTX toxin kills host cells only after contact of the bacteria with host cells, *Cell. Microbiol.*, 2008, **10**(4), 848–862, DOI: 10.1111/J.1462-5822.2007.01088.X.

74 C. S. Kim, E. H. Bae, S. K. Ma and S. W. Kim, Severe septicemia, necrotizing fasciitis, and peritonitis due to *Vibrio vulnificus* in a patient undergoing continuous ambulatory peritoneal dialysis: A case report, *BMC Infect. Dis.*, 2015, **15**(1), 1–4, DOI: 10.1186/S12879-015-1163-X/PEER-REVIEW.

75 N. Lerstloompleephunt, T. Tantawichien and V. Sitprija, Renal failure in *Vibrio vulnificus* infection, *Renal Failure*, 2000, **22**(3), 337–343, DOI: 10.1081/JDI-100100877.

76 J. Wang, X. Weng, Y. Weng, Q. Xu, Y. Lu and Y. Mo, Clinical features and treatment outcomes of *Vibrio vulnificus* infection in the coastal city of Ningbo, China, *Front. Microbiol.*, 2023, **14**, 1220526, DOI: 10.3389/FMICB.2023.1220526/BIBTEX.

77 J. W. Kronstad and M. Caza, Shared and distinct mechanisms of iron acquisition by bacterial and fungal pathogens of humans, *Front. Cell. Infect. Microbiol.*, 2013, **3**, 80, DOI: 10.3389/FCIMB.2013.00080.

78 U. Abbasi, S. Abbina, A. Gill and J. N. Kizhakkedathu, Development of an iron overload HepG2 cell model using ferrous ammonium citrate, *Sci. Rep.*, 2023, **13**(1), 21915, DOI: 10.1038/S41598-023-49072-7.

79 T. Matsuoka, M. Abe and H. Kobayashi, Iron metabolism and inflammatory mediators in patients with renal dysfunction, *Int. J. Mol. Sci.*, 2024, **25**, 3745, DOI: 10.3390/IJMS25073745.

80 W. Tan, V. Verma, K. Jeong, *et al.*, Molecular characterization of vulnibactin biosynthesis in *Vibrio vulnificus* indicates the existence of an alternative siderophore, *Front. Microbiol.*, 2014, **5**, 1, DOI: 10.3389/FMICB.2014.00001.

81 R. L. Gonciarz, E. A. Collisson and A. R. Renslo, Ferrous iron–dependent pharmacology, *Trends Pharmacol. Sci.*, 2020, **42**(1), 7, DOI: 10.1016/J.TIPS.2020.11.003.

82 Y. Chen, F. Wu, H. Pang, J. Tang, S. Cai and J. Jian, Superoxide dismutase B (*sodB*), an important virulence factor of *Vibrio alginolyticus*, contributes to antioxidative stress and its potential application for live attenuated vaccine, *Fish Shellfish Immunol.*, 2019, **89**, 354–360, DOI: 10.1016/J.FSI.2019.03.061.

83 L. Cavinato, E. Genise, F. R. Luly, E. G. D. Domenico, P. Del Porto and F. Ascenzioni, Escaping the phagocytic oxidative burst: The role of SodB in the survival of *Pseudomonas aeruginosa* within macrophages, *Front. Microbiol.*, 2020, **11**, 326, DOI: 10.3389/FMICB.2020.00326/FULL.

84 L. C. Ristow and R. A. Welch, Hemolysin of uropathogenic *Escherichia coli*: A cloak or a dagger?, *Biochim. Biophys. Acta, Biomembr.*, 2016, **1858**(3), 538–545, DOI: 10.1016/J.BBAMEM.2015.08.015.

85 H. J. Yoo, S. Lee and D. Y. Ryu, Role of the ApxIB/ApxID exporter in secretion of the ApxII and ApxIII toxins in *Actinobacillus pleuropneumoniae*, *Korean J. Vet. Res.*, 2020, **60**(4), 225–228, DOI: 10.14405/KJVR.2020.60.4.225.

